Measurement of the cosmic ray energy spectrum above 10^{18} eV using the Pierre Auger Observatory

F. Schüssler* for the Pierre Auger Collaboration†

* *Karlsruhe Institute of Technology, Karlsruhe, Germany*
† *Observatorio Pierre Auger, Av. San Martin Norte 304, 5613 Malargüe, Argentina*

Abstract. **The flux of cosmic rays above 10^{18} eV has been measured with unprecedented precision using the Pierre Auger Observatory. Two analysis techniques have been used to extend the spectrum downwards from 3×10^{18} eV, with the lower energies being explored using a novel technique that exploits the hybrid strengths of the instrument. The systematic uncertainties, and in particular the influence of the energy resolution on the spectral shape, are addressed. The spectrum can be described by a broken power-law of index 3.3 below the ankle which is measured at $\lg(E_{\rm ankle}/{\rm eV}) = 18.6$. Above the ankle the spectrum is described by a power-law $\propto E^{-2.6}$ and a flux suppression with $\lg(E_{1/2}/{\rm eV}) = 19.6$.**

Keywords**: Auger Energy Spectrum**

I. INTRODUCTION

Two independent techniques are used at the Pierre Auger Observatory to study extensive air showers created by ultra-high energy cosmic rays in the atmosphere, a ground array of more than 1600 water-Cherenkov detectors and a set of 24 fluorescence telescopes. Construction of the baseline design was completed in June 2008. With stable data taking starting in January 2004, the world's largest dataset of cosmic ray observations has been collected over the last 4 years during the construction phase of the observatory. Here we report on an update with a substantial increase relative to the accumulated exposure of the energy spectrum measurements reported in [1] and [2].

Due to its high duty cycle, the data of the surface detector are sensitive to spectral features at the highest energies. Its energy scale is derived from coincident measurements with the fluorescence detector. A flux suppression around $10^{19.5}$ eV has been established based on these measurements [1] in agreement with the HiRes measurement [3].

An extension to energies below the threshold of $10^{18.5}$ eV is possible with the use of hybrid observations, i.e. measurements with the fluorescence detectors in coincidence with at least one surface detector. Although statistically limited due to the duty-cycle of the fluorescence detectors of about 13%, these measurements make it possible to extend the energy range down to 10^{18} eV and can therefore be used to determine the position and shape of the ankle at which the power-law index of the flux changes [4], [5], [6], [7]. A precise measurement of this feature is crucial for an understanding of the underlying phenomena. Several phenomenological models with different predictions and explanations of the shape of the energy spectrum and the cosmic ray mass composition have been proposed [8], [9], [10].

II. SURFACE DETECTOR DATA

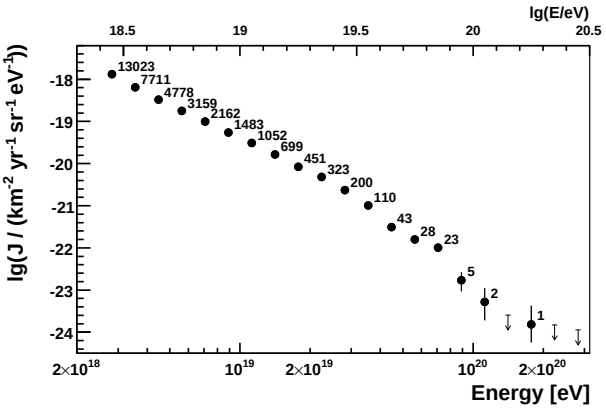

Fig. 1. Energy spectrum derived from surface detector data calibrated with fluorescence measurements. Only statistical uncertainties are shown.

The surface detector array of the Pierre Auger Observatory covers about $3000\,{\rm km}^2$ of the Argentinian Pampa Amarilla. Since its completion in June 2008 the exposure is increased each month by about $350\,{\rm km}^2\ {\rm sr\ yr}$ and amounts to $12,790\,{\rm km}^2\ {\rm sr\ yr}$ for the time period considered for this analysis (01/2004 - 12/2008). The exposure is calculated by integrating the number of active detector stations of the surface array over time. Detailed monitoring information of the status of each surface detector station is stored every second and the exposure is determined with an uncertainty of 3 % [1].

The energy of each shower is calibrated with a subset of high quality events observed by both the surface and the fluorescence detectors after removing attenuation effects by means of a constant-intensity method. The systematic uncertainty of the energy cross-calibration is 7% at 10^{19} eV and increases to 15% above 10^{20} eV [11].

Due to the energy resolution of the surface detector data of about 20%, bin-to-bin migrations influence the

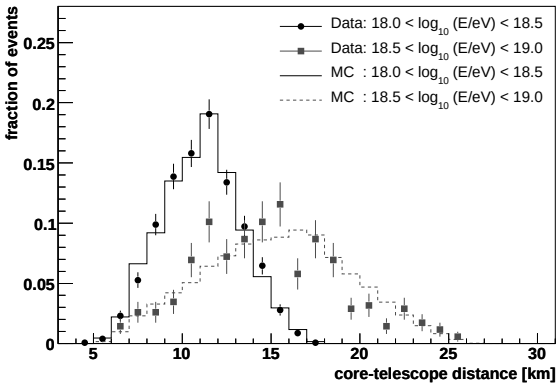

Fig. 2. Comparison between hybrid data and the Monte Carlo simulations used for the determination of the hybrid exposure.

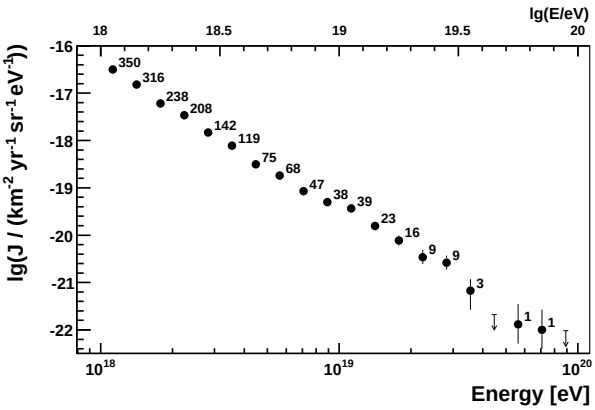

Fig. 3. Energy spectrum derived from hybrid data. Only statistical error bars are shown.

reconstruction of the flux and spectral shape. To correct for these effect, a simple forward- folding approach was applied. It uses MC simulations to determine the energy resolution of the surface detector and derive the bin-to-bin migration matrix. The matrix is then used to derive a flux parameterisation that matches the measured data after forward-folding. The ratio of this parameterisation to the folded flux gives a correction factor that is applied to data. The correction is energy dependent and less than 20% over the full energy range.

The derived energy spectrum of the surface detector is shown in Fig. 1 together with the event numbers of the underlying raw distribution. Combining the systematic uncertainties of the exposure (3%) and of the forward folding assumptions (5%), the systematic uncertainties of the derived flux is 5.8%.

III. Fluorescence detector data

The fluorescence detector of the Pierre Auger Observatory comprises 24 telescopes grouped in 4 buildings on the periphery of the surface array. Air shower observations of the fluorescence detector in coincidence with at least one surface detector permit an independent measurement of the cosmic ray energy spectrum. Due to the lower energy threshold of the fluorescence telescopes, these 'hybrid' events allow us to extend the range of measurement down to $10^{18}\,\mathrm{eV}$.

The exposure of the hybrid mode of the Pierre Auger Observatory has been derived using a Monte Carlo method which reproduces the actual data conditions of the observatory including their time variability [12]. Based on the extensive monitoring of all detector components [13] a detailed description of the efficiencies of data-taking has been obtained. The time-dependent detector simulation is based on these efficiencies and makes use of the complete description of the atmospheric conditions obtained within the atmospheric monitoring program [14]. For example, we consider only time intervals for which the light attenuation due to aerosols has been measured and for which no clouds have been detected above the observatory [15].

As input to the detector simulation, air showers are simulated with CONEX [16] based on the Sibyll 2.1 [17] and QGSJetII-0.3 [18] hadronic interaction models, assuming a $50\% - 50\%$ mixture of proton and iron primaries. Whereas the derived exposure is independent of the choice of the hadronic interaction model, a systematic uncertainty is induced by the unknown primary mass composition. After applying restrictions to the fiducial volume [19], the systematic uncertainty related to the primary mass composition is 8% at $10^{18}\,\mathrm{eV}$ and becomes negligible above $10^{19}\,\mathrm{eV}$ (see [12] for details).

Additional requirements limit the maximum distance between air shower and the fluorescence detector. They have been derived from comparisons between data and simulated events and assure a saturated trigger efficiency of the fluorescence detector and the independence of the derived flux from the systematic uncertainty of the energy reconstruction. In addition, events are only selected for the determination of the spectrum if they meet certain quality criteria [12], which assure an energy resolution of better than 6% over the full energy range.

Extensive comparisons between simulations and cosmic ray data are performed at all reconstruction levels. An example is the agreement between data and MC in the determination of the fiducial distance shown in Fig. 2. Additional cross-checks involve laser shots fired into the field of view of the fluorescence telescopes from the Central Laser Facility [20]. They have been used to verify the accuracy of the duty cycle.

The design of the Pierre Auger Observatory with its two complementary air shower detection techniques offers the chance to validate the full MC simulation chain and the derived hybrid exposure using air shower observations themselves. Based on this end-to-end verification, the calculated exposure has been corrected by 4%. The total systematic uncertainty of the derived hybrid spectrum is 10% at $10^{18}\,\mathrm{eV}$ and decreases to about 6% above $10^{19}\,\mathrm{eV}$.

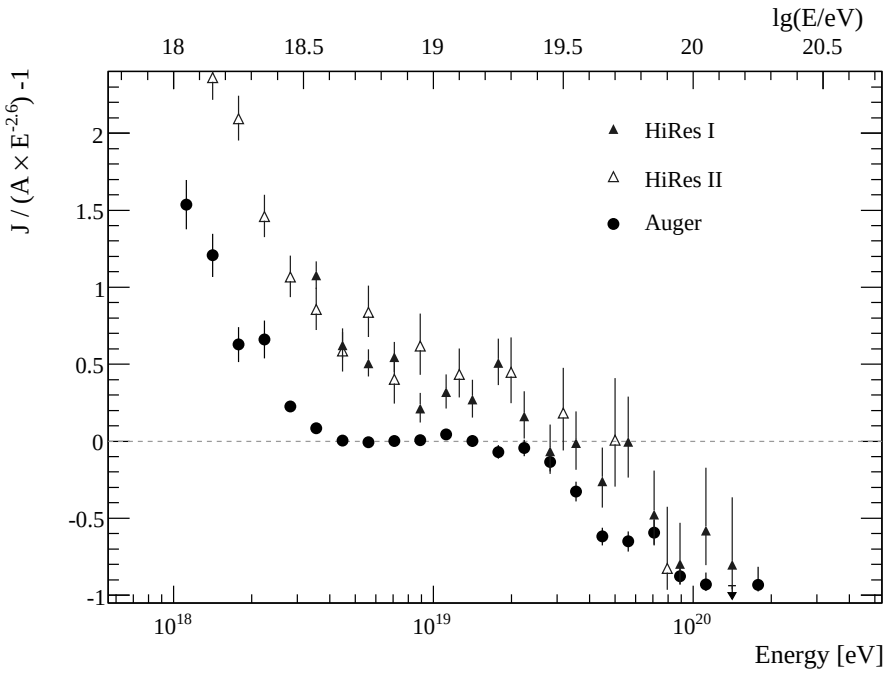

Fig. 4. The fractional difference between the combined energy spectrum of the Pierre Auger Observatory and a spectrum with an index of 2.6. Data from the HiRes instrument [3], [21] are shown for comparison.

The energy spectrum derived from hybrid measurements recorded during the time period 12/2005 - 05/2008 is shown in Fig. 3.

IV. The combined energy spectrum

The Auger energy spectrum covering the full range from $10^{18}\,\mathrm{eV}$ to above $10^{20}\,\mathrm{eV}$ is derived by combining the two measurements discussed above. The combination procedure utilises a maximum likelihood method which takes into account the systematic and statistical uncertainties of the two spectra. The procedure applied is used to derive flux scale parameters to be applied to the individual spectra. These are $k_{\mathrm{SD}} = 1.01$ and $k_{\mathrm{FD}} = 0.99$ for the surface detector data and hybrid data respectively, showing the good agreement between the independent measurements. The systematic uncertainty of the combined flux is less than 4%.

As the surface detector data are calibrated with hybrid events, it should be noted that both spectra share the same systematic uncertainty for the energy assignment. The main contributions to this uncertainty are the absolute fluorescence yield (14%) and the absolute calibration of the fluorescence photodetectors (9.5%). Including a reconstruction uncertainty of about 10% and uncertainties of the atmospheric parameters, an overall systematic uncertainty of the energy scale of 22% has been estimated [11].

The fractional difference of the combined energy spectrum with respect to an assumed flux $\propto E^{-2.6}$ is shown in Fig. 4. Two spectral features are evident: an abrupt change in the spectral index near $4\,\mathrm{EeV}$ (the "ankle") and a more gradual suppression of the flux beyond about $30\,\mathrm{EeV}$.

Some earlier measurements from the HiRes experiment [3], [21] are also shown in Fig. 4 for comparison. A modest systematic energy shift applied to one or both experiments could account for most of the difference between the two. The spectral change at the ankle appears more sharp in our data.

The energy spectrum is fitted with two functions. Both are based on power-laws with the ankle being characterised by a break in the spectral index γ at E_{ankle}. The first function is a pure power-law description of the spectrum, i.e. the flux suppression is fitted with a spectral break at E_{break}. The second function uses a smooth transition given by

$$J(E; E > E_{\mathrm{ankle}}) \quad \propto \quad E^{-\gamma_2} \, \frac{1}{1 + \exp\left(\frac{\lg E - \lg E_{1/2}}{\lg W_c}\right)}$$

in addition to the broken power-law to describe the ankle. This fit is shown as black solid line in Fig. 5. The derived parameters (quoting only statistical uncertainties) are:

In Fig. 5 we show a comparison of the combined energy spectrum with spectral shapes expected from different astrophysical scenarios. Assuming for example a uniform distribution of sources, no cosmological evolution of the source luminosity ($(z+1)^m$, i.e. $m = 0$) and a source flux following $\propto E^{-2.6}$ one obtains a spectrum that is at variance with our data. Better agreement is obtained for a scenario including a strong cosmological evolution of the source luminosity ($m = 5$) in combi-

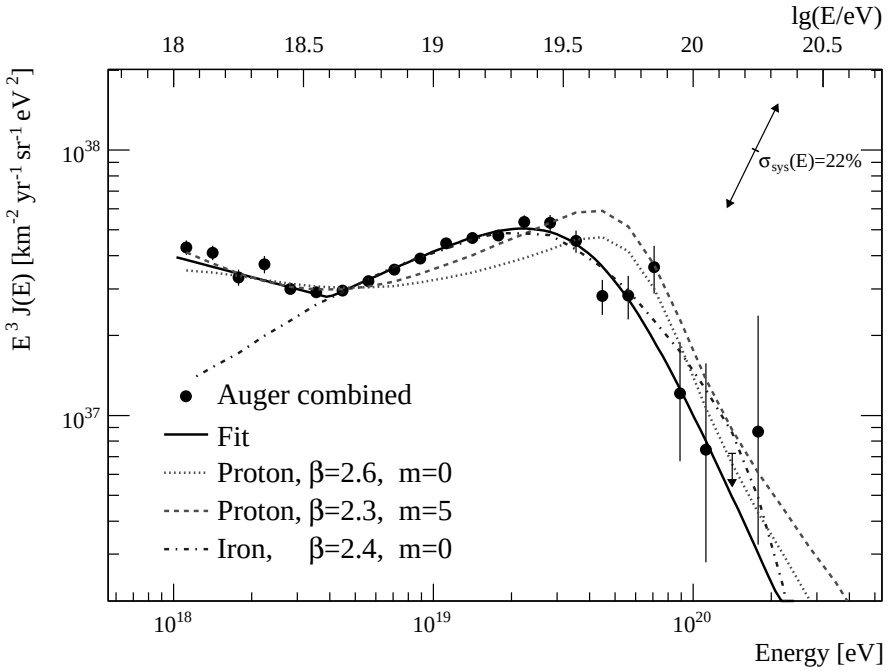

Fig. 5. The combined energy spectrum compared with several astrophysical models assuming a pure composition of protons (red lines) or iron (blue line), a power-law injection spectrum following $E^{-\beta}$ and a maximum energy of $E_{\rm max} = 10^{20.5}\,{\rm eV}$. The cosmological evolution of the source luminosity is given by $(z+1)^m$. The black line shows the fit used to determine the spectral features (see text). A table with the flux values can be found at [22].

parameter	broken power laws	power laws + smooth function
$\gamma_1 (E < E_{\rm ankle})$	3.26 ± 0.04	3.26 ± 0.04
$\lg(E_{\rm ankle}/{\rm eV})$	18.61 ± 0.01	18.60 ± 0.01
$\gamma_2 (E > E_{\rm ankle})$	2.59 ± 0.02	2.55 ± 0.04
$\lg(E_{\rm break}/{\rm eV})$	19.46 ± 0.03	
$\gamma_3 (E > E_{\rm break})$	4.3 ± 0.2	
$\lg(E_{1/2}/{\rm eV})$		19.61 ± 0.03
$\lg(W_{\rm c}/{\rm eV})$		0.16 ± 0.03

nation with a harder injection spectrum ($\propto E^{-2.3}$). A hypothetical model of a pure iron composition injected with a spectrum following $\propto E^{-2.4}$ and uniformly distributed sources with $m = 0$ is able to describe the measured spectrum above the ankle, below which an additional component is required.

V. SUMMARY

We presented two independent measurements of the cosmic ray energy spectrum with the Pierre Auger Observatory. Both spectra share the same systematic uncertainties in the energy scale. The combination of the high statistics obtained with the surface detector and the extension to lower energies using hybrid observations enables the precise measurement of both the ankle and the flux suppression at highest energies with unprecedented statistics. First comparisons with astrophysical models have been performed.

REFERENCES

[1] J. Abraham et al. (Pierre Auger Collaboration). *Physical Review Letters*, 101:061101, 2008.
[2] L. Perrone for the Pierre Auger Collaboration. *Proc. 30th Int. Cosmic Ray Conf. (Merida, Mexico)*, 4:331, 2007.
[3] R. U. Abbasi et al. *Physical Review Letters*, 100:101101, 2008.
[4] J. Linsley. *Proc of 8th Int. Cosmic Ray Conf., Jaipur*, 4:77–99, 1963.
[5] M. A. Lawrence, R. J. O. Reid, and A. A. Watson. *J. Phys.*, G17:733–757, 1991.
[6] M. Nagano et al. *J. Phys.*, G18:423–442, 1992.
[7] D. J. Bird et al. *Phys. Rev. Lett.*, 71:3401–3404, 1993.
[8] V. Berezinsky, A. Z. Gazizov, and S. I. Grigorieva. *Phys. Lett.*, B612:147–153, 2005.
[9] A. M. Hillas. *J. Phys.*, G31:R95–R131, 2005.
[10] T. Wibig and A. W. Wolfendale. *J. Phys.*, G31:255–264, 2005.
[11] C. Di Giulio for the Pierre Auger Collaboration. *Proc. 31th Int. Cosmic Ray Conf. (Lodz, Poland)*, 2009.
[12] F. Salamida for the Pierre Auger Collaboration. *Proc. 31th Int. Cosmic Ray Conf. (Lodz, Poland)*, 2009.
[13] J. Rautenberg for the Pierre Auger Collaboration. *Proc. 31th Int. Cosmic Ray Conf. (Lodz, Poland)*, 2009.
[14] S. BenZvi for the Pierre Auger Collaboration. *Proc. 31th Int. Cosmic Ray Conf. (Lodz, Poland)*, 2009.
[15] L. Valore for the Pierre Auger Collaboration. *Proc. 31th Int. Cosmic Ray Conf. (Lodz, Poland)*, 2009.
[16] T. Bergmann et al. *Astroparticle Physics*, 26:420–432, 2007.
[17] R. Engel et al. *Proc. 26th Int. Cosmic Ray Conf. (Salt Lake City, USA)*, 415, 1999.
[18] S. Ostapchenko. *Nucl. Phys. B (Proc. Suppl.)*, 151:143, 2006.
[19] M. Unger for the Pierre Auger Collaboration. *Proc 30th Int. Cosmic Ray Conf., Merida*, 4:373, 2007.
[20] B. Fick et al. *JINST*, 1:P11003, 2006.
[21] R. U. Abbasi et al. *Phys. Lett.*, B619:271–280, 2005.
[22] http://www.auger.org/combined_spectrum_icrc09.txt